Proceedings Paper:

Scott, M., Sims, N.D., Green, P.L. et al. (2 more authors) (2014) Sensitivity Analysis of an Advanced Gas-Cooled Reactor Control Rod Model. In: Proceedings of ISMA 2014, International Conference on Noise and Vibration Engineering. ISMA 2014, International Conference on Noise and Vibration Engineering, 15-17 Sep 2014, Leuven, Belgium. .

Sensitivity Analysis of an Advanced Gas-Cooled Reactor Control Rod Model

M. Scott[1], P. L. Green[1], C. Grant-Wilson[2], M. Bateman[2], K. Worden[1], N. D. Sims[1]
[1] Dynamics Research Group, Department of Mechanical Engineering, University of Sheffield, Mappin Street, Sheffield S1 3JD, UK
e-mail: **mea08ms@sheffield.ac.uk**

[2] EDF Energy, Barnett Way, Barnwood, Gloucester, GL4 3RS

Abstract

A model has been made of the primary shutdown system of an Advanced Gas-cooled Reactor nuclear power station. The aim of this paper is to explore the use of sensitivity analysis techniques on this model. The two motivations for performing sensitivity analysis are to quantify how much individual uncertain parameters are responsible for the model output uncertainty, and to make predictions about what could happen if one or several parameters were to change. Global sensitivity analysis techniques were used based on Gaussian process emulation; the software package GEM-SA was used to calculate the *main effects*, the *main effect index* and the *total sensitivity index* for each parameter and these were compared to local sensitivity analysis results. The results suggest that the system performance is resistant to adverse changes in several parameters at once.

1 Introduction

The United Kingdom has seven Advanced Gas-cooled Reactor nuclear power stations (AGRs), which provide around 20% of its electricity. The AGR design was developed in the 1970s and is unique to Britain. The primary shutdown mechanism is provided by the control rods which absorb the neutrons needed to sustain a chain reaction of uranium fissions in the reactor core. The control rods are continually raised and lowered in order to maintain a critical reaction. A reactor typically has around 80 control rods, each with its own actuator. Should the reactor exceed its normal operating conditions, the control rods will be released by an electromagnetic clutch and insert into the core under gravity, shutting down the reactor. This system was designed experimentally and is regularly tested to ensure the rods will enter the core quickly enough to shutdown the reactor with a sufficient safety margin. Large amounts of collected data and modern modelling techniques give an opportunity to understand and monitor the primary shut down system performance at a more detailed level; this is beneficial for managing the plant commercially and for giving early warning of any potential performance issues. The objective of this paper is to develop a mathematical model of the system and explore the use of probabilistic sensitivity analysis techniques on this model.

Sensitivity analysis is concerned with how a model's inputs affect its output. In the context of modelling control rods there are two main uses for sensitivity analysis. The first is to investigate how the uncertainty of individual model parameters is responsible for the uncertainty of the model output. This is useful when developing and refining the model as effort can be focused on the most important parameters. The second use for sensitivity analysis is for making predictions about the effects of changing parameters on the performance of the system, i.e. what will be the effect on model output if one or several model parameters deviate from their original values?

It is relatively straightforward to assess the local sensitivity of a model to its parameters, by partially differentiating the model output with respect to different parameters. However this method is not particularly informative because it fails to take into account nonlinear responses. A slightly more informative technique is to run the model for a range of parameter values, keeping the others constant. Both of these methods fail to take into account the fact that sensitivity to a parameter could vary as other parameters change. For a model with many parameters assessing the effects of all possible parameter combinations is challenging [1]. Global sensitivity analysis techniques investigate the entire range of the possible input space using statistical methods; these can be time consuming and still require careful interpretation.

Monte Carlo analysis can be used to sample from the probability distribution of model outputs, given a set of probability distributions of model inputs, these output distributions can be used to infer global sensitivity qualities [2, 3]. Whilst this is effective, it can be extremely computationally expensive, especially if there are many parameters of interest. A way of reducing the expense of global sensitivity analysis given a computationally expensive model is to use a surrogate model - a model of a model. This still requires many model runs but far fewer than Monte Carlo analysis. A technique based on Fourier amplitude sensitivity testing (FAST) provides an elegant way of estimating the contribution of input uncertainty to output uncertainty, however this method is limited to investigating the main effects of parameters and does not give information regarding interactions. [4, 5].

Choosing sensitivity analysis techniques requires a compromise between robustness, computational cost, ease of implementation and conceptual simplicity. Within the nuclear industry, robustness is generally preferred at the expense of computational cheapness, to within reason [6]. In the current case, the purpose of the model and sensitivity measures is to assist in decision making and increase understanding of the system. It is desirable that the meaning of the measures used and the concepts behind them are sufficiently intuitive that someone with little knowledge of sensitivity analysis is able to confidently use them.

The technique chosen in this investigation is a Bayesian approach to surrogate modelling developed in [7], which will be introduced in more detail below. It was chosen as it is both computationally efficient and robust, and although the maths behind it is relatively complicated the basic principles are not difficult to understand.

2 The model

A schematic of the system of interest is shown in Figure 1 and a more detailed sketch of the brake system is given in Figure 2. The governor shaft is connected to the motor by an electromagnetic clutch (not shown). If power to the clutch is lost then the governor shaft will be released and the rods will insert into the core. A two-stage braking mechanism is attached to the governor shaft. The primary brake is driven by flyweights and is dependent on the rod velocity. The secondary brake is driven by a lead screw, which is connected to the bevel shaft by gears (not shown). Key assumptions made during the derivation of the model structure are:

- The effects of the chain friction, bearing friction, gear/sprocket efficiency and the friction between the side walls of the core and the rods are lumped together in a single, scaled friction parameter F_f which acts as a constant force resisting the rod motion.
- The coefficient of friction between the governor and the brake is a constant.
- The drag forces from the gas are directly proportional to the velocity of the rods and do not depend on the displacement.
- All components are assumed to be fully rigid, except the springs in the brake mechanism.

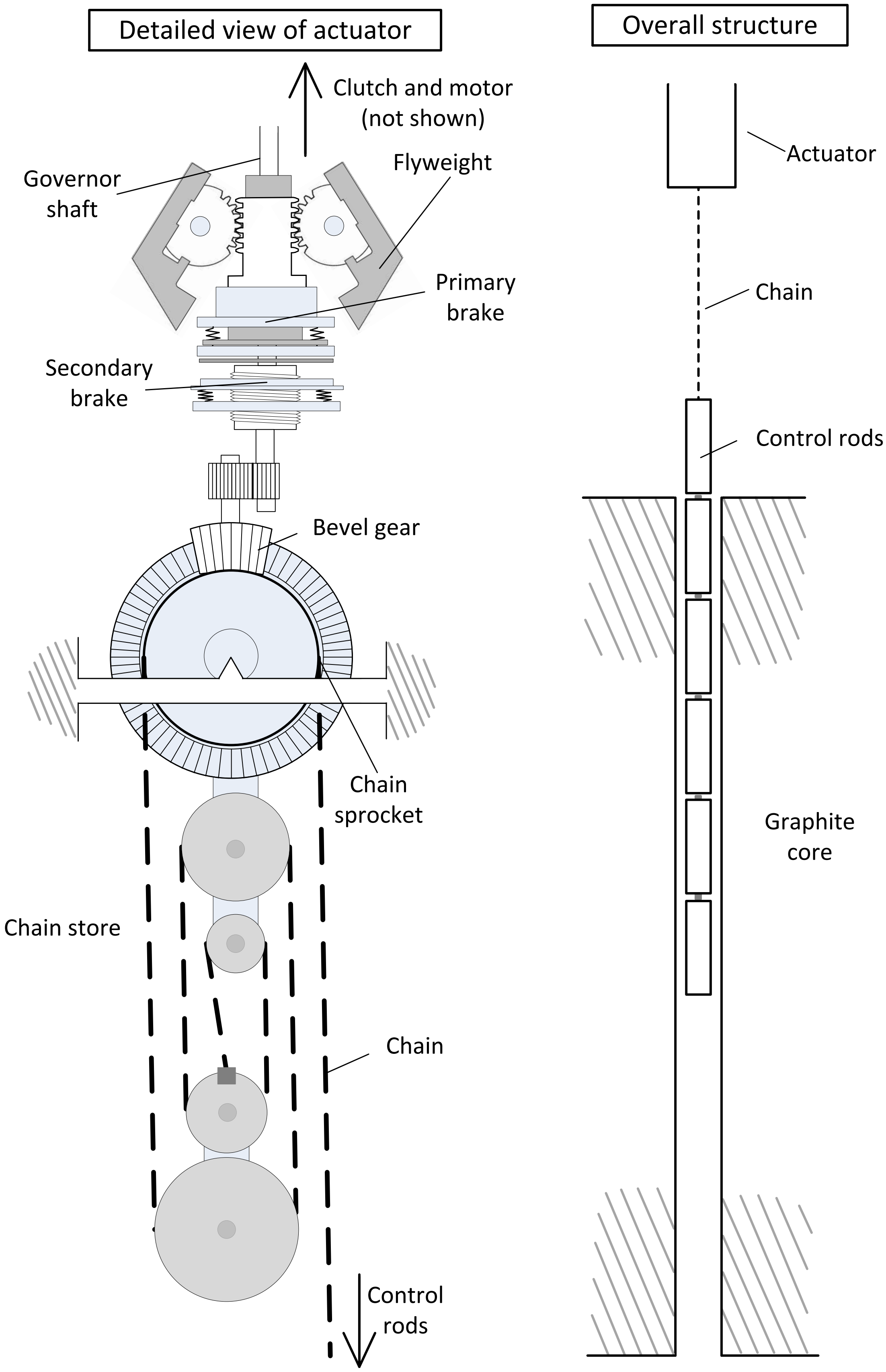

Figure 1: Schematic of control rod system.

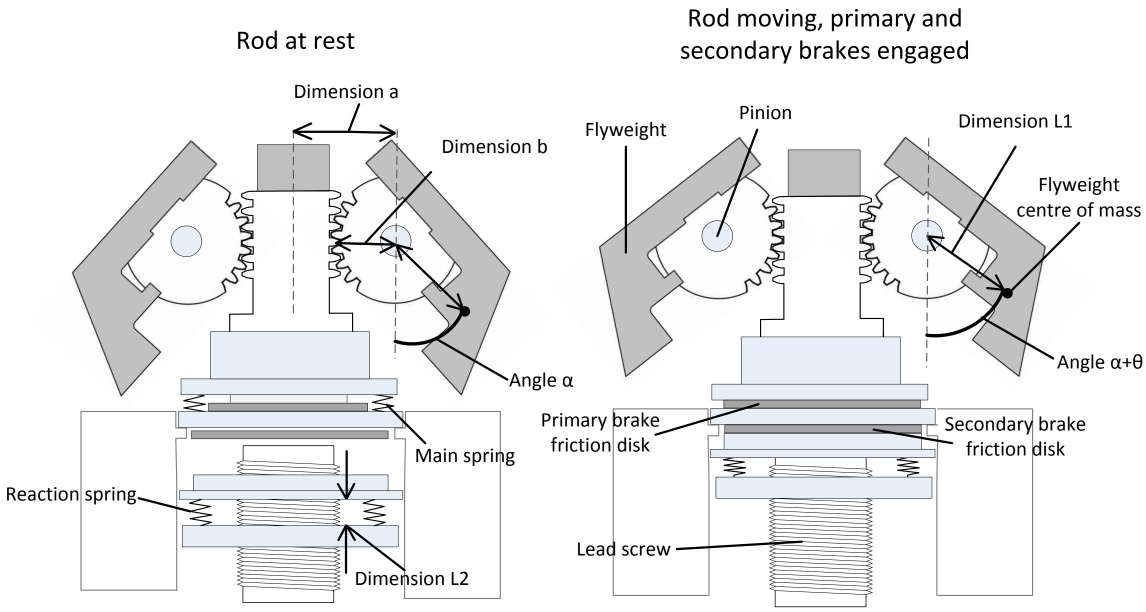

Figure 2: The primary and secondary brake mechanisms.

The action of the brake is sufficiently complicated that there are 9 distinct stages of rod motion. Each stage is described by 2 simultaneous differential equations, one for the motion of the rods and one for the motion of the flyweights. The points at which the model transitions between stages are dictated by the position of the flyweights and the rods. The equations describing stage 6 of the rod's motion are given as an example below.

The rod acceleration, $\ddot{\boldsymbol{x}}$, is given by:

$$\ddot{\boldsymbol{x}} = \frac{Mg + M_c g\boldsymbol{x} - h\dot{\boldsymbol{x}} - F_f - (C_1\dot{\boldsymbol{x}}^2 - C_8\boldsymbol{\theta_f} - C_9) - (C_{10} + C_{11}\boldsymbol{\theta_f} + C_{12}\boldsymbol{x})}{M + M_c\boldsymbol{x} + I} \tag{1}$$

Where:

$$\begin{aligned}
c =& L_1 \sin(\alpha + \boldsymbol{\theta_f}) \\
d =& L_1 \cos(\alpha + \boldsymbol{\theta_f}) \\
C_8 =& \mu R b(k + k_1) \\
C_9 =& \mu R(Mfgc/b + C_b - M_p g) \\
C_{10} =& \mu R k_2(i_c + L_2 - x_{ubrake} - b\theta_{fmax}) \\
C_{11} =& \mu R k_2 b \\
C_{12} =& \mu R k_2 C_r
\end{aligned}$$

The acceleration of the flyweights is given by:

$$\ddot{\boldsymbol{\theta}}_{\boldsymbol{f}} = \frac{C_a\dot{\boldsymbol{x}}^2 - M_f gc - (kb\boldsymbol{\theta_f} - M_p g)b - F_u \mathrm{sgn}(\dot{\boldsymbol{\theta}}_{\boldsymbol{f}}) - (k_1 b\boldsymbol{\theta_f} + C_b)b - (C_5 + C_6\boldsymbol{\theta_f} + C_7 x)}{(I_f + M_t b^2)} \tag{2}$$

Where:

$$\begin{aligned}
C_5 =& k_2 b(i_c + L_2 - x_{ubrake} - b\theta_{fmax}) \\
C_6 =& k_2 b^2 \\
C_7 =& k_2 b C_r
\end{aligned}$$

Parameter	Description	Estimated using	Expected value
$M\ (kg)$	Mass of control rods.	Acurately known	173
$M_c\ (kg/m)$	Mass of chain.	3D drawings	2.0
$L1\ (m)$	Dimension (see fig 2).	3D drawings	0.016
$L2\ (m)$	Dimension (see fig 2).	3D drawings	0.027
$a\ (m)$	Dimension (see fig 2).	3D drawings	0.021
$b\ (m)$	Dimension (see fig 2).	3D drawings	0.013
$\mu\ (Nm/N)$	Brake coefficient of friction.	System ID	8.1
$k_1\ (N/m)$	Main spring stiffness.	System ID	184000
$k_2\ (N/m)$	Reaction spring stiffness.	System ID	12300
$k\ (N/m)$	Return spring stiffness.	System ID	860
$\theta_{fspring}\ (degrees)$	Flyweight angle when thrust block comes into contact with main spring.	3D drawings	7.9
$\theta_{fmax}\ (degrees)$	Flyweight angle when primary brake engages.	3D drawings	8.1
$\theta_{fbrake2}\ (degrees)$	Flyweight angle when secondary brake fully engaged.	3D drawings	-8.5
$h\ (N/m/s)$	Viscous drag coefficient.	System ID	36
$Ff\ (N)$	Combined friction force.	System ID	330
$Fu\ (Nm)$	Friction resisting flyweight movement.	System ID	0.45
$I\ (kgm)$	Combined scaled rotational inertia of all rotating components.	3D drawings	240
$R\ (radians/m)$	Ratio of governor shaft rotation to rod movement.	Acurately known	190
$M_p\ (kg)$	Combined mass of the thrust bearing, thrust block and upper faceplate.	3D drawings	1.6
$M_t\ (kgm)$	Combined mass of the 3 faceplates, friction disks, thrust bearing and thrust block.	3D drawings	2.8
$I_f\ (kgm)$	Rotational inertia of flyweights about pinion.	3D drawings	0.00030
$M_f\ (kg)$	Mass of flyweights.	3D drawings	0.89
$n_0\ (m)$	Initial compression of main spring.	3D drawings	0.018
$i_c\ (m)$	Initial compression of reaction springs.	3D drawings	0.017
C_r	Ratio of leadscrew movement to rod movement.	Acurately known	0.003
$x_{brake}\ (m)$	Rod position when secondary brake first engages.	Acurately known	6.2
$\alpha\ (degrees)$	Flyweight angle when rod is at rest.	3D drawings	55

Table 1: Description and expected value of model parameters.

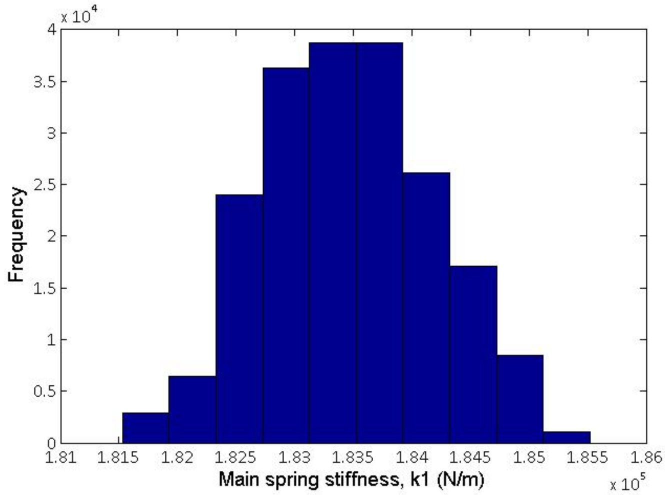

Figure 3: Histogram of k1 probability distribution.

The model relies on 28 parameters which represent physical attributes of the system e.g. spring stiffnesses, masses, coefficients of friction etc. These parameters are listed in Table 1. Some of the parameters (the gear ratios and the mass of the rods) are accurately known quantities. Many of the parameters were estimated using 3D models of the system which are fairly accurate, but their accuracy cannot be guaranteed. There were some parameters which are not possible to measure directly or estimate analytically with any accuracy. These were the friction terms, spring stiffnesses, and the viscous drag coefficient.

The system is tested regularly and time histories of the rod positions have been recorded. The possible values of the unknown parameters were estimated using Bayesian system identification, which combines prior knowledge of the parameters with measured data from the system to give probability distributions of parameter values. An example of this is given in Figure **??**, which shows the probability distribution for the stiffness of the primary brake main spring, $k1$. The data used was a single time history taken from the insertion test of a newly maintained system. A plot of this time history is given in Figure **??** alongside a plot of the modelled rod position (the model used the mean of the estimated parameter probability distributions for the unknown parameter values). Describing the details of Bayesian system identification is outside the scope of this paper, the techniques used here were developed in [8] and [9].

The sensitivity analysis methods used in this investigation require the model to give a single value output. The value chosen here is the distance the rod has inserted 4.5 seconds after it has been released, which was chosen as it is used as a key measure of how well the primary shutdown system is performing. The design specification is that the rods must have inserted at least 6.5m after 4.5 seconds to shutdown the reactor with a sufficient safety margin. It is desirable that the rods enter the core as quickly as possible, while not traveling fast enough to cause any damage.

3 Bayesian Sensitivity analysis

3.1 The Emulator

The sensitivity analysis technique used here involves the use of an emulator - a model of the model. The model is treated as an unknown function, with the possible ranges of the input parameters specified by probability distributions. A selection of input vectors are sampled from these distributions, using a Maximin Latin Hypercube design to ensure complete, even coverage of the input space. The model is then run using these

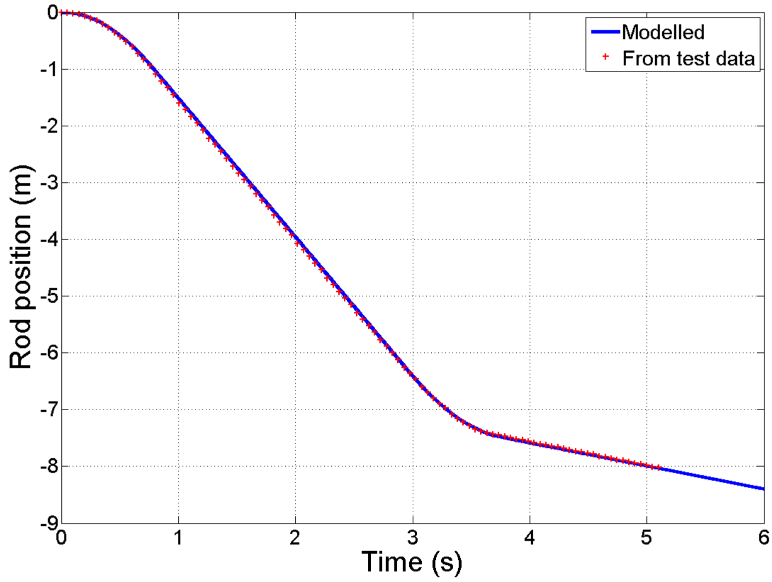

Figure 4: Plot of measured rod position and modelled rod position during an insertion test.

vectors as inputs to provide the training data for creating the emulator.

If it is assumed that the model is a smooth function of its inputs, then a response surface can be fitted to the training data using a least squares regression and the output can be estimated for any set of inputs. Early use of emulators in sensitivity analysis involved using the response surface to perform Monte Carlo analysis at a reduced cost [3]. In the current case the response surface is used to provide the mean of the multivariate Gaussian probability distribution which represents the prior belief in the value of the model output. The prior distribution is then conditioned on the training data to give a posterior distribution over functions, which can be used to infer many global sensitivity values, the ones of interest will be described below. This technique is described in detail in [7].

3.2 Main effects and interactions

The model output, y can be decomposed into main effects and interactions of its input parameters, $\mathbf{x}$ ($\mathbf{x}$ denotes the vector of n input parameters $\{x_1, ..., x_n\}$)

$$y = E(Y) + \sum_{i=1}^{n} z_i(x_i) + \sum_{i<j} z_{i,j}(x_{i,j}) \sum_{i<j<k} z_{i,j,k}(x_{i,j,k}) + ... + z_{i,j,k}(\mathbf{x}) \tag{3}$$

where,

$$z_i(x_i) = E(Y|x_i) - E(Y) \tag{4}$$

$$z_{i,j}(x_{i,j}) = E(Y|x_i, j) - z_i(x_i) - z_j(x_j) - E(Y) \tag{5}$$

$$z_{i,j,k}(x_{i,j,k}) = E(Y|x_i, j, k) - z_{i,j}(x_{i,j}) - z_{i,k}(x_{i,k}) - z_{j,k}(x_{j,k}) - z_i(x_i) - z_j(x_j) - z_k(x_k) \tag{6}$$

$z_i(x_i)$ is the main effect of x_i, $z_{i,j}(x_{i,j})$ is the first order interaction between x_i and x_j, $z_{i,j,k}(x_{i,j,k})$ is the second order interaction etc. Y is the random variable corresponding to the function output, $E(Y)$ is the expected value of the output considering all possible combinations of inputs.

Parameter	Range	Main effect index (%)	Total sensitivity index (%)
Mass of flyweights (kg)	$0.8 - 0.98$	3.6	4.1
Angle - alpha (degrees)	$50 - 60$	11.1	12.1
Dimension - L1 (m)	$0.0144 - 0.0176$	7.5	8.3
Dimension a (m)	$0.0189 - 0.0231$	1.1	1.3
Dimension b (m)	$0.0117 - 0.0143$	4.0	4.5
Brake coefficient of friction (Nm/N)	$0.02 - 0.032$	52.23	55.37
Reaction spring stiffness N/m	$11000 - 13000$	4.7	5.9
Initial compression of main spring (m)	$0.0164 - 0.02$	2.5	2.9
Initial compression of reaction springs (m)	$0.0153 - 0.0187$	5.1	8.3

Table 2: Main effect index and total sensitivity index values for most important parameters from the first run of sensitivity analysis.

The main effect of a parameter is the output of the model with the parameter held constant, averaged over all of the other parameters' possible values. This can be plotted over the parameter's possible range and gives a good visual representation of the model's sensitivity to that parameter. A plot of the interactions shows the effect of varying two or more parameters simultaneously (in addition to their main effects) averaged over the rest of the parameter space.

3.3 Variance based measures

The variance of the main effect is known as the *main effect index* (MEI) and it can be written as,

$$\mathrm{MEI_i} = \mathrm{var}\{E(Y|X_i)\} \tag{7}$$

This is the expected amount that the uncertainty of the model output would be reduced if the true value of x_i was known.

The *total sensitivity index* (TSI) is the variance caused by a parameter and any interaction involving that parameter,

$$\mathrm{TSI_i} = \mathrm{var}(Y) - \mathrm{var}\{E(Y|X_{-i})\} \tag{8}$$

It can also be thought of as the remaining variance if the true values of all of the parameters except x_i are known ($-i$ refers to the complement of the subset i).

For a more detailed description of these measures, and how they are inferred see [7] and [10].

4 Results and discussion

4.1 The first run of sensitivity analysis

When performing global sensitivity analysis, choosing the shape and width of the parameter distributions is important. Choosing an incorrectly wide distribution means that a parameter's importance could be overestimated and an incorrectly narrow one would underestimate importance. Without a quantitative knowledge of uncertainty in the parameter values, engineering judgement is required in choosing the width of the distributions and it is worth keeping this in mind when interpreting the results. All of the parameters are assumed to have uniform distributions.

The purpose of the first run of sensitivity analysis performed here is to investigate how the uncertainty in individual model parameters is responsible for the uncertainty of the model output. This can be used to decide which parameters are most important when developing the model, as well as giving insight into how the system behaves. There are 25 parameters which were investigated here out of 28 in total. The mass of the rods, the gear ratios and the gravitational constant are all known accurately and are not going to change. 18 of the parameters were measured from 3D drawings of the system which are thought to be reasonably accurate. For these parameters a range of $\pm 10\%$ either side of the parameter's expected value was used, which is likely to be far in excess of the actual inaccuracy. Probability distributions for the other 7 parameters were estimated using Bayesian system identification, however these distributions were estimated assuming that the other parameter values were accurate, so the ranges used have been doubled.

At this point it is worth noting the difference between subjective and objective uncertainty in parameter values. Subjective uncertainty results from a lack of accurate knowledge of the system, e.g. a dimension which is not accurately known. Objective uncertainty results from the fact that some elements in the system behave in a stochastic way, for instance, brake pad friction coefficients have been shown to vary unpredictably [11].

The MEIs and TSIs of the parameters which were responsible for more than 1% of the output variance are shown in Table 2. It can be seen that more than half of the output variance arises from the brake friction term μ. It is also clear from the table that the vast majority of the variance arises from the main effects of parameters, since the values of the MEIs are close to the values of the TSIs. The sum of the MEIs is 95%, so interactions account for only around 5% of the output variance.

Plots of the main effects for selected parameters are shown in Figure 5 to 8. Alongside these are plots of the model output with all of the parameters held at their expected values, except the parameter of interest which is varied across a range of values. It should be noted that the y-axis limits are not the same on the main effects plots and the corresponding *one-at-a-time* (1AAT) plots. A common theme across all of the parameters is that the expected model outputs from the main effects plots are higher (the rod has inserted further) than the corresponding model output from the 1AAT plots. This is because on average the model is more sensitive to the change in a parameter when it increases the distance the rod inserts than when it decreases it. This can be seen in Figure 7 which shows that the output is more sensitive to a decrease in brake friction than an increase. The fact that the system is generally less sensitive to parameters when they slow down the rod's insertion suggests that the system is more likely to remain safe, but it is not the case for all parameters.

Figure 8 shows that plotting the main effects can obscure a local nonlinearity in the response to a change in a parameter. While in the current case the model is fairly insensitive to the parameter, it does highlight the fact that when looking at the global behaviour it is possible to miss details in the local behaviour.

4.2 The second run of sensitivity analysis

The purpose of the second run was to investigate what could happen if parameters were to change. Only four parameters were investigated; the brake friction coefficient μ, the general friction term F_f, the main spring stiffness and the reaction spring stiffness. These parameters were chosen because they could feasibly change during the lifetime of the reactor, and because the model was not shown to be totally insensitive to them during the first run of sensitivity analysis. The authors currently do not have quantitative information regarding how these parameters could change, so the ranges chosen are speculative. Each parameter was varied, from its expected value in the direction that would have a detrimental effect on the systems performance, i.e. which would slow the speed of the rod's insertion.

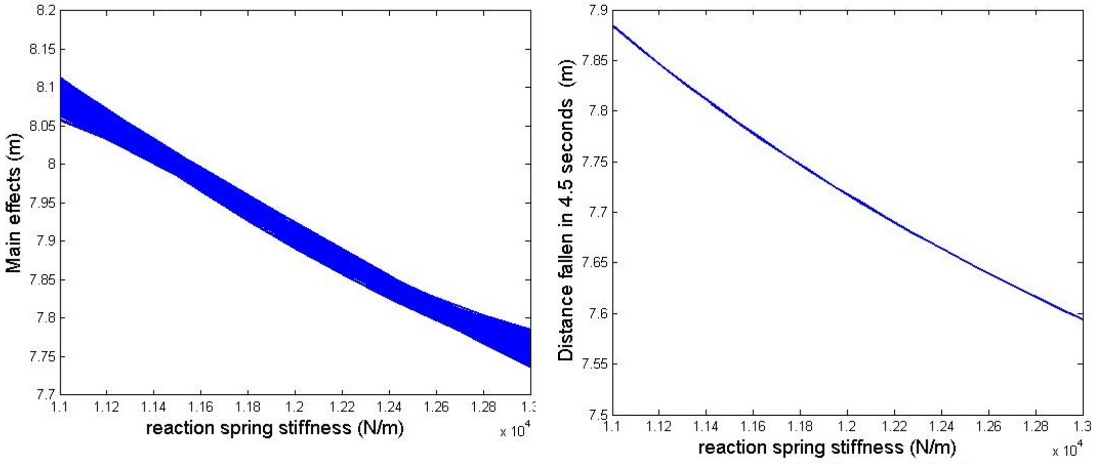

Figure 5: Main effect plot and one at a time plot for the reaction spring stiffness.

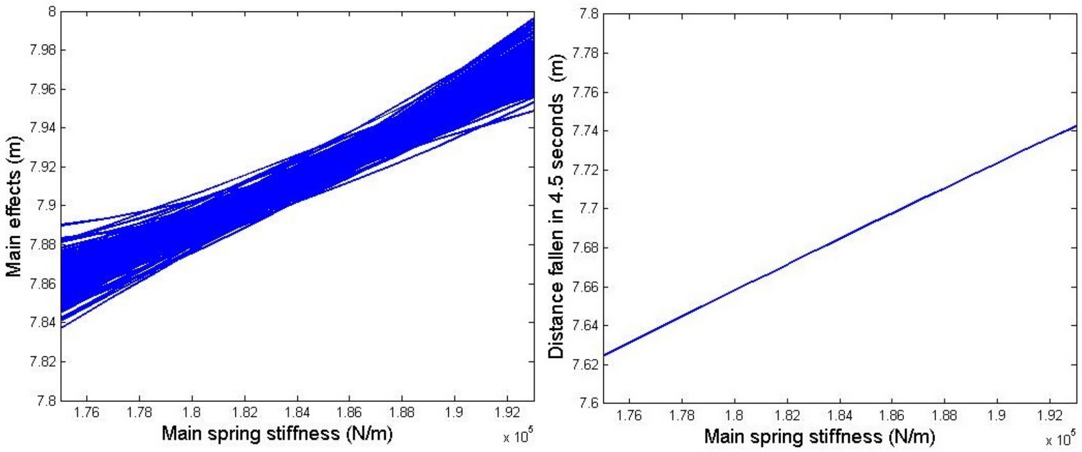

Figure 6: Main effect plot and one at a time plot for the main spring stiffness.

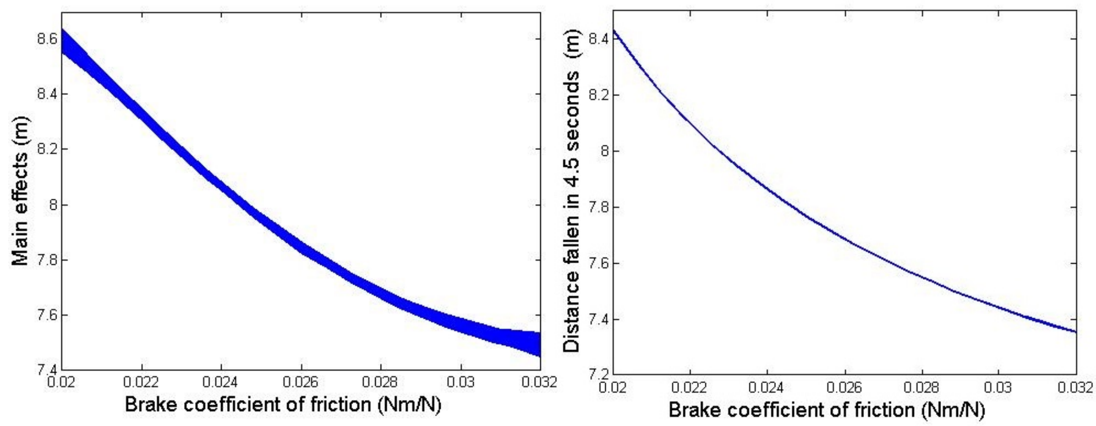

Figure 7: Main effect plot and one at a time plot for the brake friction coefficient.

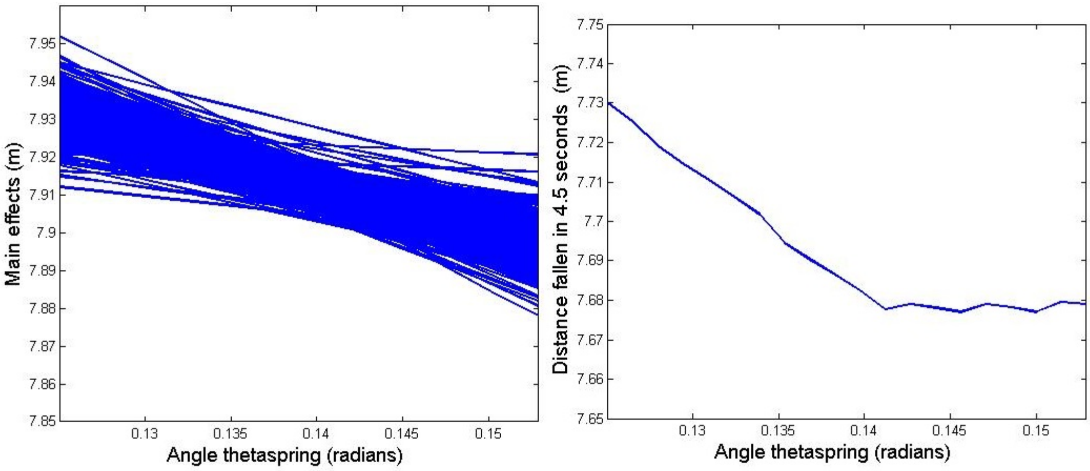

Figure 8: Main effect plot and one at a time plot for the angle ”thetaspring”.

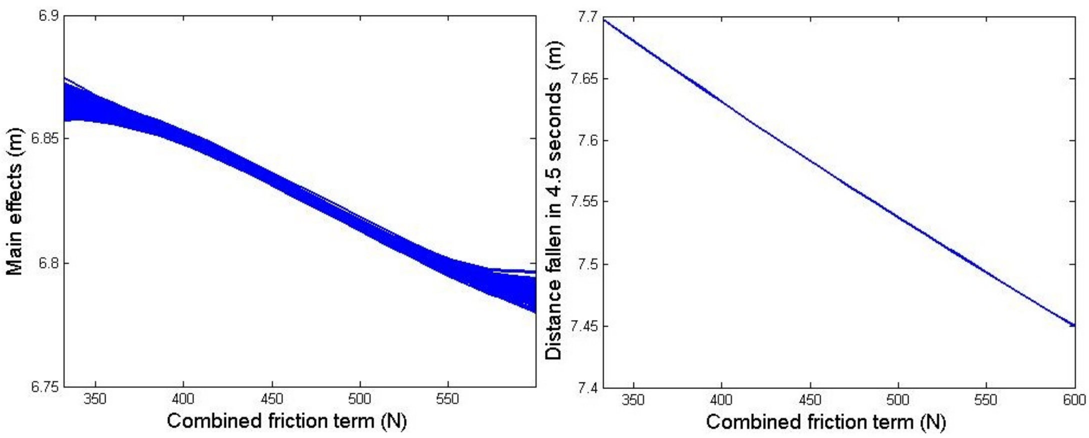

Figure 9: Extended main effect plot and one at a time plot for the combined friction force.

Table 3 shows the MEIs and TSIs from the second run of sensitivity analysis where fewer parameters were considered with an extended range. Again it can be seen that there is a relatively small contribution from the interactions. The results suggest that the most influential parameters are the brake friction coefficient and the main spring stiffness. However, it is not known how likely these parameters are to change, and by how much; it is not possible to truly state which are the most influential parameters without this information.

Figures 9 to 12 show the main effects and 1AAT plots. The main effects show the rod inserting less far than the 1AAT plots. This is to be expected since the main effects are the outputs averaged over the other parameters ranges, and the other parameters are varied from their expected values in the direction which slows the rod's insertion. The main effects plots also show much lower sensitivity to each of the parameters compared to the 1AAT plots. This shows that if parameters change causing the rod drop to become slower, then the system will become less sensitive to other parameters changing. This suggests that unless a component drastically fails, the system is likely to stay safe.

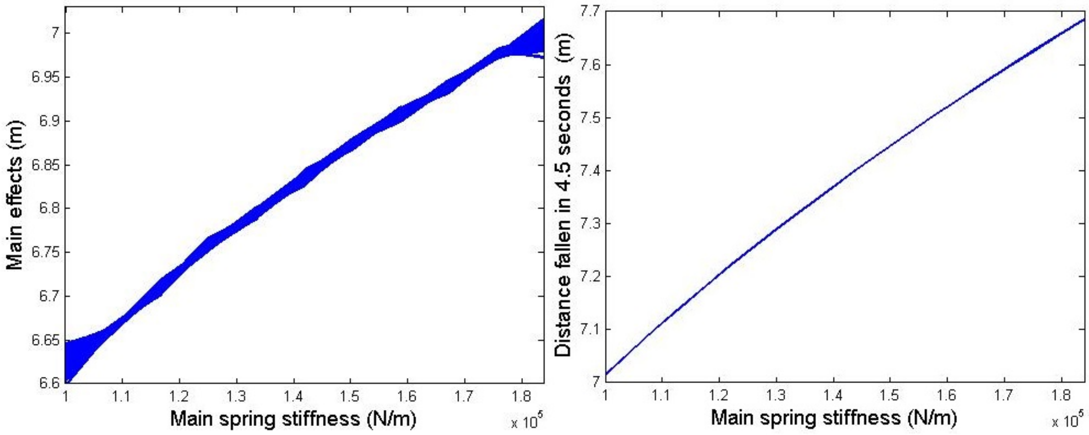

Figure 10: Extended main effect plot and one at a time plot for the main spring stiffness.

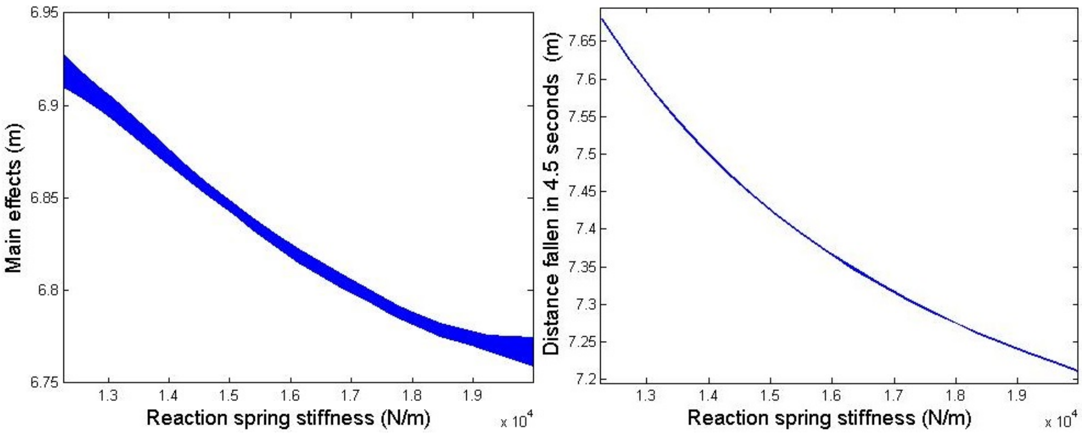

Figure 11: Extended main effect plot and one at a time plot for the reaction spring stiffness.

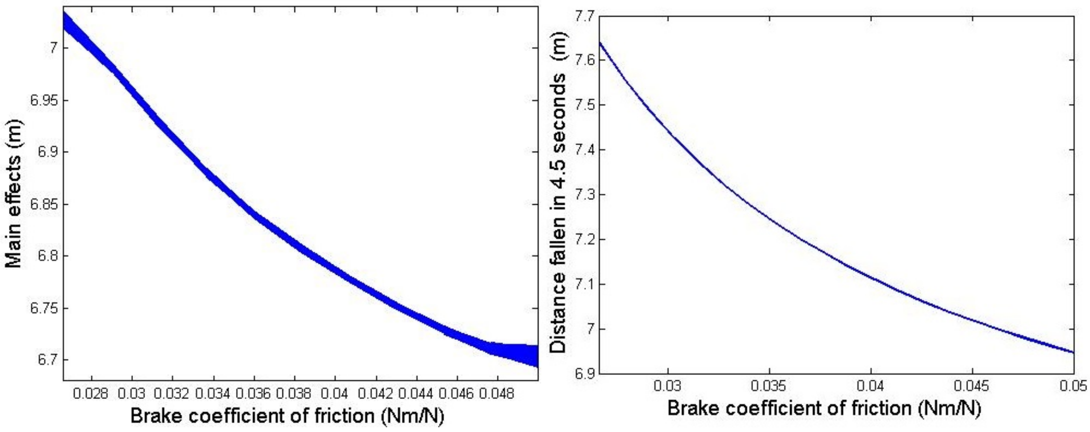

Figure 12: Extended main effect plot and one at a time plot for the brake friction coefficient.

Parameter	Range	Main effect index (%)	Total sensitivity index (%)
Brake coefficient of friction (Nm/N)	$0.026 - 0.05$	37.4	40.2
Reaction spring stiffness (N/m)	$12000 - 20000$	8.5	10.5
Combined friction term (N)	$330 - 600$	2.4	3.34
Main spring stiffness (N/m)	$100000 - 184000$	48.12	50.61

Table 3: Main effect index and total sensitivity index values from the second run of sensitivity analysis.

5 Conclusions

The aim of this paper was to develop a model of the AGR primary shutdown system and explore the use of probabilistic sensitivity analysis techniques on this model, with the objective of shedding light on the contribution of parameters to model uncertainty and the system's performance. The results suggest that gaining a better understanding of the brake friction would be the most effective way of reducing the model uncertainty. However, it is impossible to definitively characterise the uncertainty of the model output without accurate estimates for how uncertain the input parameter values are. The results from the second round of sensitivity analysis imply that the system ought to be resistant to changes in several parameters at once; a component's properties would have to change dramatically before the system becomes unsafe.

It is made clear in these results that while these global sensitivity analysis techniques use information from the entire range of the possible parameter space, they do not fully describe the model's sensitivity to these parameters, because details (such as nonlinearities) can be lost when averaging over the other possible parameters. This study has shown that it can be useful to show local sensitivity analysis results alongside the global ones as it provides context for comparison.

6 Acknowledgments

The Author would like to thank EDF Energy for funding the project and Marc Kennedy from the University of Sheffield Probability and Statistics Department for the use of GEM-SA.

References

[1] A. Saltelli, K. Chan, and E. M. Scott. *Sensitivity Analysis*. Wiley, 2000.

[2] P. Doubilet, C.B. Begg, M.C. Weinstein, P. Braun, and B.J. McNeil. Probabilistic sensitivity analysis using Monte Carlo simulation: A practical approach. *Med Decis Making.*, 5:157–177, 1985.

[3] J. Helton. Uncertainty and sensitivity analysis techniques for use in performance assessment for radioactive waste disposal. *Reliability Engineering and System Safety*, 42:327–367, 1993.

[4] G.J. McRae, J. W. Tilden, and J. H. Seinfeld. Global sensitivity analysis-a computational implementation of the Fourier amplitude sensitivity test (FAST). *Computers & Chemical Engineering*, 6(1):15–25, 1982.

[5] A. Saltelli, S. Tarantola, and K. P.-S. Chan. A quantitative model-independent method for global sensitivity analysis of model output. *Technometrics*, 41:39–56, 1999. ISSN 0040-1706.

[6] M.E. Pati Cornell. Probability and uncertainty in nuclear safety decisions. *Nuclear Engineering and Design*, 93:319–327, 1986.

[7] J. Oakley and A. O'Hagan. Probabilistic sensitivity analysis of complex models: a Bayesian approach. *Journal of the Royal Statistical Society, Series B*, 66:751–769, 2002.

[8] P. L. Green. Bayesian system identification of nonlinear dynamical systems using a fast MCMC algorithm. *European Nonlinear Oscillations Conference*, 2014.

[9] P. L. Green and T. Baldacchino. Bayesian system identification in structural dynamics: Annealing with constant entropy variation. *Probabilistic Engineering Mechanics (Under Review)*, 2014.

[10] K. Worden and W. Becker. On the identification of hysteretic systems. part ii: Bayesian sensitivity analysis. *Mechanical Systems and Signal Processing*, 29:213–227, 2012.

[11] G. P. Ostermeyer. On the dynamics of the friction coefficient. *Wear*, 254:852–858, 2003.